

ORIGINAL ARTICLE

Adult ovarian granulosa cell tumor transcriptomics: prevalence of FOXL2 target genes misregulation gives insights into the pathogenic mechanism of the p.Cys134Trp somatic mutation

BA Benayoun^{1,2,6,7}, M Anttonen^{3,4,7}, D L'Hôte^{1,2}, M Bailly-Bechet⁵, N Andersson⁴, M Heikinheimo⁴ and RA Veitia^{1,2}

Ovarian granulosa cell tumors (OGCT) are the most frequent kind of sex cord-stromal tumors, and represent ~2–5% of all ovarian malignancies. OGCTs exist as two entities, juvenile and adult types, with specific clinical and pathological characteristics. The molecular pathogenesis of these tumors has just begun to be unraveled. Indeed, recent studies have indicated that mutation and/or misregulation of the key ovarian transcription factor FOXL2 has a role in OGCT formation, although the mechanisms remain unclear. To better understand the molecular characteristics of OGCT, we studied the transcriptomic profiles of ten human adult-type OGCT samples, as well as ethnically matched granulosa cell (GC) controls. We find that the OGCT samples analyzed herein exhibit several hallmarks of cancer, including increased expression of genes linked to cell proliferation, but decreased expression of those conferring sensitivity to cell death. Moreover, genes differentially expressed in OGCTs are significantly enriched for known FOXL2 target genes, consistently with the prevalence of FOXL2 somatic mutation in these tumors. Expression of these targets is altered in a way expected to promote malignant transformation, for instance, through induction of genes associated with faster cell cycling and downregulation of genes associated with cell death. Over time, such defects may be responsible at least partly for the malignant transformation of healthy GCs into OGCT. These insights into the molecular pathogenesis of OGCTs may open the way to new efforts in the development of more targeted therapeutic strategies for OGCT patients.

Oncogene (2013) 32, 2739–2746; doi:10.1038/onc.2012.298; published online 16 July 2012

Keywords: FOXL2; ovarian granulosa cell tumor; ovary; transcriptome

INTRODUCTION

Ovarian granulosa cell tumors (OGCT) are the most frequent sex cord-stromal tumors, and represent ~2–5% of ovarian cancers.¹ There are two distinct types of OGCTs, the juvenile and adult forms, which display different clinical and histopathological features.² OGCTs are usually low-grade malignancies, but the patients have a high risk of recurrent disease occurring up to 40 years after primary tumor resection.^{1,3} Reliable clinical and molecular prognostic markers remain to be discovered, because the molecular pathogenesis of OGCT remains unclear. Indeed, common cancer aggressivity markers (such as status of *P53* or *cMYC*) have no prognostic value for this disease.^{1,4}

Recent studies have revealed that a somatic *FOXL2* mutation leading to the p.Cys134Trp substitution is a feature shared by over 95% of adult-type OGCTs, which has been suggested to constitute an early event in their pathogenesis.^{5–9} *FOXL2* encodes a transcription factor of the Forkhead superfamily, and its germline mutations are responsible for a human genetic disease, the Blepharophimosis Ptosis Epicanthus-inversus Syndrome.¹⁰ *FOXL2* is expressed in the somatic granulosa cells (GCs) of the ovary during development and throughout female fertile life, and has a key role in maintaining ovarian identity.^{11,12} In GCs, *FOXL2* has been linked to the regulation of several key cellular

processes, such as apoptosis, oxidative stress response and cell proliferation.^{13–16}

Investigations of the molecular effects of the p.Cys134Trp *FOXL2* mutation have given molecular clues on its impact in OGCT pathogenesis. Indeed, transactivation activity measured by luciferase assays has suggested that the mutation could disturb a functional interaction between *FOXL2* with its partner *SMAD3*.⁵ Recently, Kim and collaborators¹⁷ have shown that the p.Cys134Trp mutant version is severely deficient in its ability to induce apoptosis of OGCT-derived cells. Moreover, our recent results suggest that the p.Cys134Trp mutant induces a promoter-specific mild loss-of-function, notably on the promoters of target genes involved in the regulation of cell cycle progression and DNA-damage repair.¹⁵ All this has led us to hypothesize that *FOXL2* acts as a tumor suppressor.¹⁸ In contrast, one study has suggested that the mutation may also be responsible for a promoter-specific gain-of-function, notably on the ovarian promoter of the *CYP19A1* aromatase, the key enzyme responsible for estrogen synthesis.¹⁹

However, an in-depth understanding of the *in vivo* effects of the p.Cys134Trp mutation has yet to be achieved, to promote the development of potential targeted therapies. Here, we have performed a detailed study of OGCT's molecular characteristics,

¹Institut Jacques Monod, Paris, France; ²Université Paris Diderot/Paris, Paris, France; ³Department of Obstetrics and Gynecology, Helsinki University Central Hospital, Helsinki, Finland; ⁴Children's Hospital, University of Helsinki and Helsinki University Central Hospital, Helsinki, Finland and ⁵Laboratoire de Biométrie et Biologie Evolutive, Centre National de la Recherche Scientifique, UMR 5558, Université Lyon, Villeurbanne, France. Correspondence: Professor RA Veitia, Université Paris-Diderot/Paris 7 & Institut Jacques Monod, CNRS-UMR 7592, Bâtiment Buffon, 15 Rue Hélène Brion, Paris Cedex 13, France.

E-mail: veitia.reiner@ijm.univ-paris-diderot.fr

⁶Current address: Department of Genetics, Stanford University, 300 Pasteur Drive, Stanford, CA, USA

⁷These authors contributed equally to this work.

Received 15 March 2012; revised 8 June 2012; accepted 11 June 2012; published online 16 July 2012

through a transcriptomic analysis of 10 OGCT samples, in comparison with healthy GC controls. We propose that the p.Cys134Trp mutated *FOXL2* version contributes to reduced sensitivity to apoptosis and increased proliferation of GCs, which would allow their malignant transformation process.

RESULTS AND DISCUSSION

OGCT exhibit classical cancer-associated transcriptomic alterations. To unravel transcriptomic characteristics of OGCTs, we obtained ten adult-type OGCT tumor samples, as well as two ethnically matched primary GC samples derived from an IVF program, as control for transcriptomic profiling. These tumors exhibit a broad spectrum of clinical and histopathological parameters, for example, oncological staging (FIGO nomenclature), mitotic index and subtypes (Table 1). The genomic sequence status of *FOXL2* in these tumors has previously been published.⁶ They also all carry the c.402C>G/p.Cys14Trp *FOXL2* mutation at the RNA level, as seen on the cDNA sequence most frequently in a heterozygous state. However, in two cases, only the c.402C>G substitution, and not the wild-type (WT) sequence, was detected (Table 1).

Tumor cDNA samples were hybridized on high-density Roche-Nimblegen expression microarrays (two independent reverse transcriptions, pre-processing and hybridizations per RNA sample), and the signal was processed so as to obtain expression values per gene, after applying the ComBat algorithm to correct for batch effects.²⁰ Replicates for the H20 and H30 samples in the first batch did not pass Nimblegen Quality Control checks, and have been excluded from the analysis. Because of the constraints of IVF programs, human control GC samples have been exposed to FSH stimulation before collection, which might alter gene expression patterns. Alterations of FSH signaling might play a role in GCT pathogenesis, notably because pre-ovulatory growth of GCs is induced by this hormone. However, to avoid false positive hits in our analysis, we decided to remove FSH-responsive genes. Thus, we took advantage of a published dataset assessing the effects of FSH treatment on mouse primary GCs (GSE20466; $N=3$ independent replicates).²¹ Differentially regulated genes at false discovery rate of 5% were assessed using the R implementation of the SAM algorithm,²² and a list of the human orthologs was obtained using the BioMart bioinformatics portal. These genes were designated as 'FSH-responsive' and removed from further investigation in our samples to limit the bias introduced by the treatment of primary GCs. There are 16 031 non-FSH-responsive genes represented on the Nimblegen microarray design (gene-level expression normalized file available as Supplementary Table 1; the raw data has been deposited to Array Express repository under accession number E-MTAB-483).

To assess the transcriptomic similarities among OGCTs and control GC samples, we used the Pvcust algorithm,²³ an unsupervised clustering approach that uses a multiscale bootstrap resampling strategy to assess uncertainty in hierarchical cluster analysis (Figure 1a). As expected, we observed that healthy GC samples clustered together apart from OGCT samples with very good bootstrap values, and that replicate hybridizations of OGCT samples clustered mostly in pairs. Interestingly, the H28 tumor clustered away from other OGCT samples, though none of its histopathological characteristics obviously set it apart from the other samples.

To better understand the transcriptomic alterations of OGCTs, we attempted to cluster non-FSH-responsive genes into three groups depending on their expressional behavior in normal GC compared with OGCTs. Namely, the expected possible expressional behaviors of genes in OGCTs compared with GCs can be (i) consistent downregulation in GCs with respect to OGCTs, (ii) consistent upregulation or (iii) no substantial/consistent changes across studied samples. To sort the genes, we chose a K-means clustering approach, setting the number K of expected clusters to 3. The K-means clustering method allows to iteratively group genes into a set of K clusters, by attributing each gene to the cluster with the closest mean value in an unsupervised manner. Thus, by setting K to 3, and if our hypothesis is correct, we can thus expect to recover the three predicted behaviors above. The output of the clustering was analyzed using Java TreeView,²⁴ and the clusters displaying differences in behavior between control GCs and tumor samples were selected for further analysis. As expected, the algorithm grouped the genes into three homogeneous clusters corresponding to the above-mentioned cases (Figure 1a).

We identified 5821 genes with a tendency to be downregulated in OGCT samples compared with control GCs (class i) and 5651 genes with a tendency to be upregulated in the tumor samples (class ii). Functional annotation of the differentially expressed genes using the DAVID annotation portal^{25,26} revealed classical cancer characteristics (Figures 1b and c). Indeed, genes upregulated in the tumor samples were significantly associated with gene ontology (GO) terms linked to cell proliferation. On the other hand, genes with a tendency to be downregulated in OGCT samples were significantly associated with GO terms linked to cell cycle arrest and cell death. In general, increased proliferation capacities and decreased sensitivity to cell death are necessary for successful malignant transformation and are recognized as 'hallmarks' of cancer cells.^{27,28}

Additionally, the misregulation patterns that we observe here are most likely not due to the exclusion of FSH-responsive genes from the analysis, as very similar clustering patterns and enrichments for functional annotations of differentially regulated

Table 1. Histo-pathological characteristics of RNA from healthy GC and adult OGCT samples studied by transcriptomics (Sample ID and details as in⁶)

| Sample ID | Patient Age | Sample type | FIGO tumor stage | <i>FOXL2</i> locus status (p.C134W) | Mitotic index | Tumor subtype |
|-----------|-------------|-------------|------------------|-------------------------------------|---------------|----------------|
| H1 | 36 | Primary | Ic | Heterozygote | Low | Differentiated |
| H4 | 73 | Recurrent | Recurrence | Homo/hemizygote | Low | Diffuse |
| H8 | 54 | Primary | Ic | Heterozygote | High | Differentiated |
| H18 | 54 | Primary | Ia | Homo/hemizygote | Low | Differentiated |
| H20 | 34 | Primary | Ia | Heterozygote | Low | Diffuse |
| H23 | 67 | Primary | II | Heterozygote | Low | Differentiated |
| H24 | 52 | Primary | Ia | Heterozygote | Low | Differentiated |
| H28 | 29 | Primary | Ic | Heterozygote | High | Differentiated |
| H30 | 56 | Primary | Ia | Heterozygote | Low | Differentiated |
| H33 | 65 | Primary | II | Heterozygote | Low | Differentiated |
| hGC1 | – | IVF primary | – | WT | – | – |
| hGC2 | – | IVF primary | – | WT | – | – |

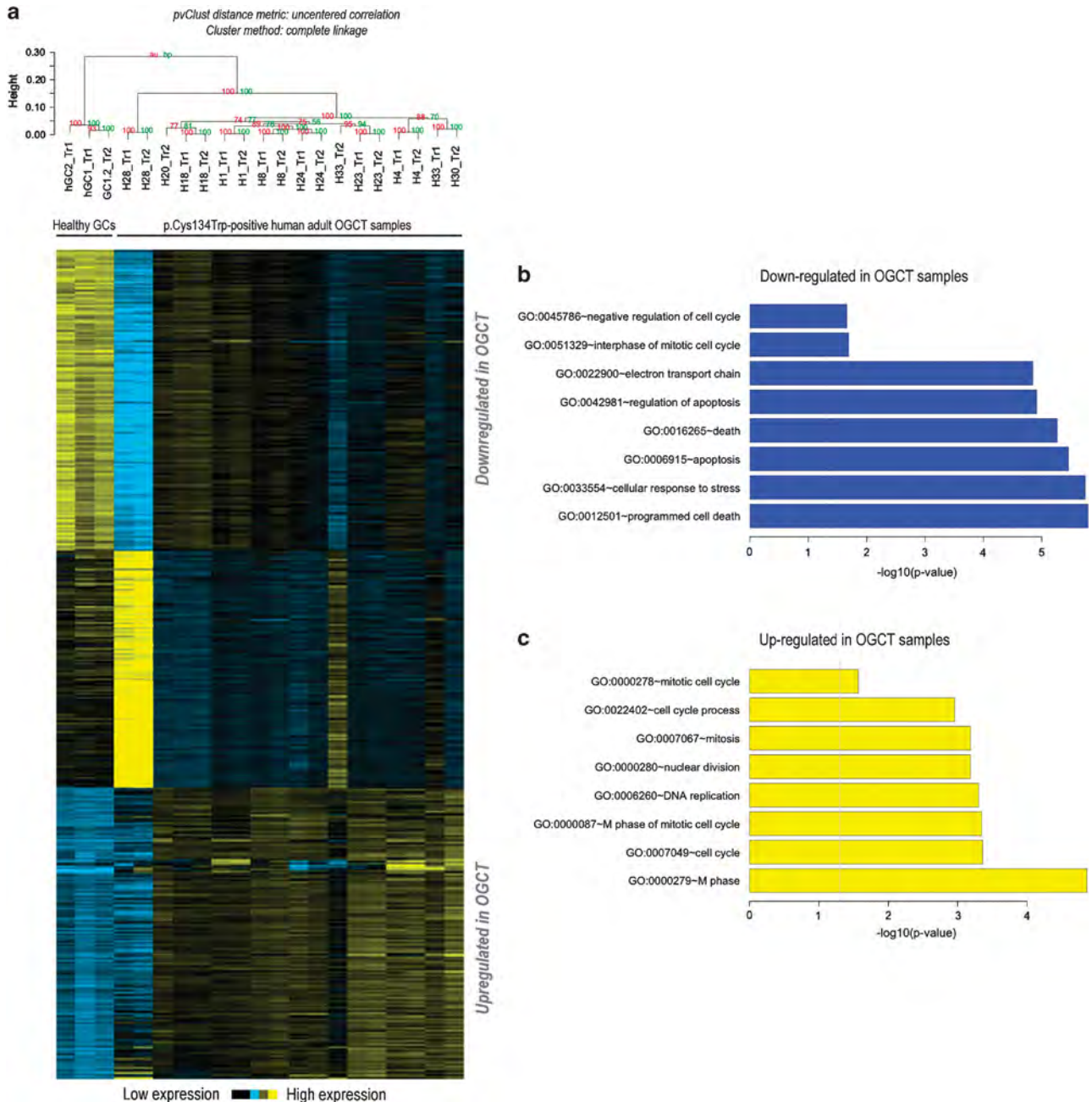


Figure 1. *K*-means clustering of transcriptome patterns of healthy GCs and OGCT samples, excluding FSH-responsive genes, reveals classical cancer characteristics. **(a)** Clustering of non-FSH responsive genes from human GC and OGCT samples. Top panel: results of pvclust clustering²³ show a clear separation of healthy GC and OGCT samples by transcriptomic data. AU/BP: confidence/Bootstrap values of dendrogram branches from pvclust. Sample names are from Table 1, 'Tr1' and 'Tr2' correspond respectively to the first and second hybridization experiments. Bottom panel: *K*-means clustering visualized using Java Treeview, with samples ordered following pvclust results. The three expected clusters of differential behavior between tumor samples and healthy cells were identified. The normalized gene expression file, used for clustering, is provided as Supplementary Table 1. **(b)** and **(c)** represent enriched GO terms for up- or downregulate gene clusters, using $-\log(P\text{-value})$ as assessed by the DAVID functional annotation software to plot their significance.^{25,26} Vertical gray lines indicate the 0.05 *P*-value significance threshold after the Bonferroni correction for multiple testing by DAVID.

genes can be observed using the full gene set (Supplementary Figure 1).

Assessing the role of FOXL2 target genes misregulation in OGCT transcriptomic alterations

As mentioned above, the somatic p.Cys134Trp FOXL2 mutation is carried by over 95% of adult-type OGCTs, at least at the

heterozygous level,⁵⁻⁹ which strongly indicates that the mutation itself is an early and necessary step during GC malignant transformation.

To assess the potential role of FOXL2 mutation/misregulation in OGCT pathogenesis, we assessed the proportion of FOXL2 targets in genes that were differentially expressed or whose expression was not altered in OGCTs. A recent high-throughput chromatin immunoprecipitation (ChIP-on-Chip)

experiment, involving immunoprecipitated material from adult-type OGCT-derived KGN cells and from a KGN clone stably overexpressing WT FOXL2 identified FOXL2 targets at a genomic scale.¹⁵

Interestingly, we find that genes differentially expressed in our human adult OGCT samples are more likely to carry significant FOXL2 CHIP-on-chip peaks in their promoter regions (Figure 2a), which clearly suggests that genes differentially expressed in OGCTs are enriched for FOXL2 direct target genes. This is both consistent and compatible

with the overwhelming frequency of FOXL2 somatic mutation in OGCT cases, and suggests that FOXL2 mutation itself may be responsible for transcriptomic alterations leading to OGCT formation.

Juvenile OGCTs are not associated with FOXL2 mutations, but a reduction of FOXL2 expression at the protein level has been detected in the most aggressive tumors.²⁹ We did not have access to human juvenile OGCT samples, but a mouse model for juvenile OGCT has been reported, carrying the triple *Smad1/5/8* genes inactivation, and transcriptomic changes in resulting tumors versus

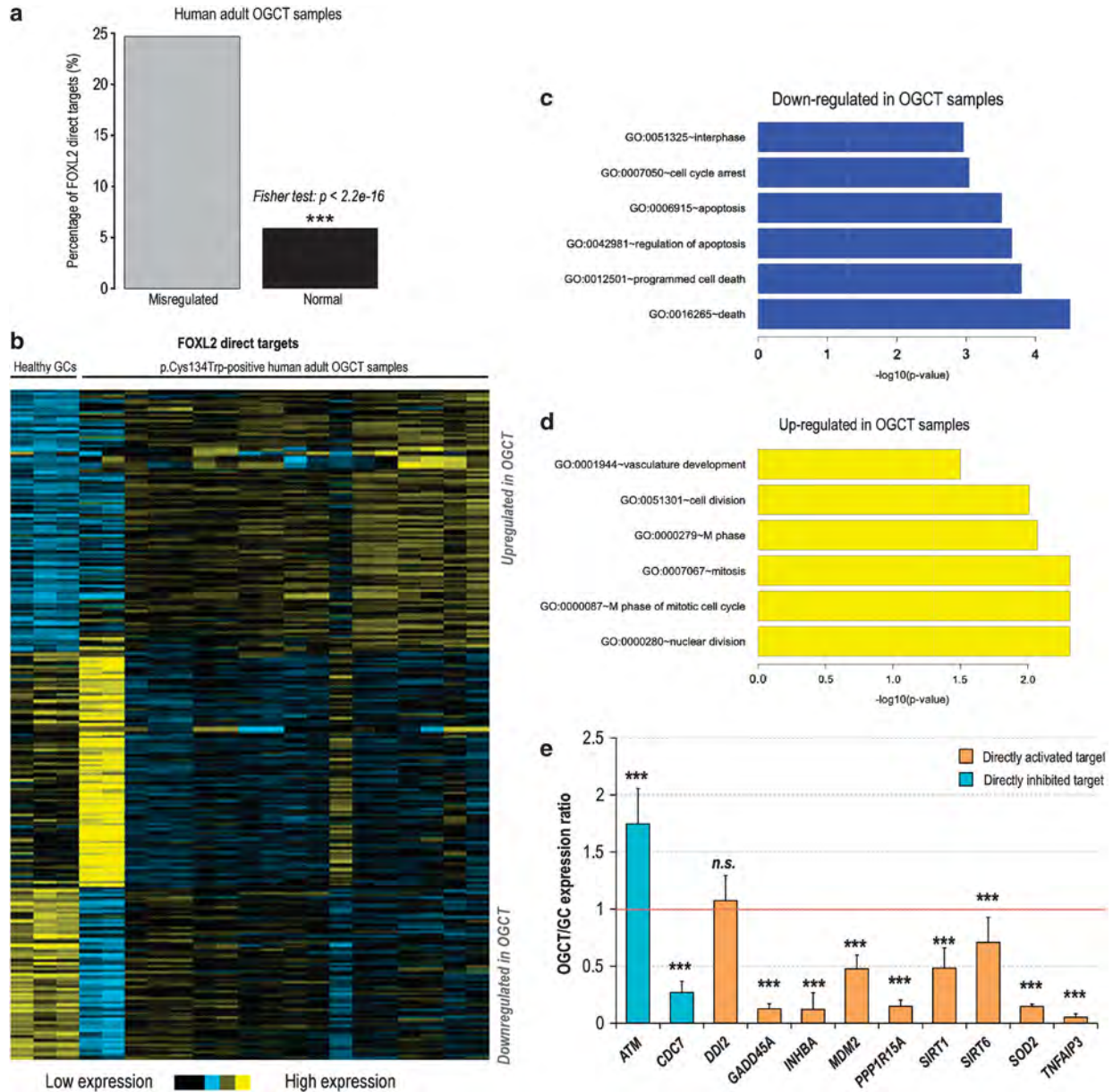


Figure 2. FOXL2 target genes misregulation in human adult OGCT samples. **(a)** Enrichment for FOXL2 binding at the promoters of genes differentially expressed in OGCT versus GC samples. The hypergeometric distribution (Fisher's exact test) was used to compute the significance of the enrichment. **(b)** Graphical output of *K*-means clustering analysis of the expressional behavior of FOXL2 direct targets performed using Cluster3.0 ($K = 3$, 500 tries, distance measure: Spearman rank correlation). Samples are in the same order as in Figure 1a. **(c)** and **(d)** Relevant GO terms enrichments in up- and down-regulated clusters, using $-\log(P\text{-value})$ as assessed by the DAVID functional annotation software to plot their significance.^{25,26} Vertical gray lines indicate the 0.05 *P*-value significance threshold after the Bonferroni correction for multiple testing by DAVID. **(e)** Ratio of all probes (that is, probe fluorescence values in OGCT over healthy GC) for 11 FOXL2 direct target genes that are insensitive to FSH. This shows the percentage of expression of the targets in OGCT as compared with the corresponding healthy tissue. Blue bars stand for genes known to be directly inhibited by FOXL2, and yellow bars for genes known to be directly activated by FOXL2. Error bars: s.d. Statistical significance in repeated one sample Student's *t*-tests for each gene (that is, comparison with respect to unchanged behavior, ratio = 1), after application of the Bonferroni correction for multiple testing on the 11 genes, $**P < 0.01$ and $***P < 0.001$. NS, not significant.

control GCs have been previously assessed by microarrays.³⁰ Interestingly, *Foxl2* transcripts are significantly downregulated in these mouse juvenile OGCT samples (Figure 3), which is consistent with previous observations of a downregulation of FOXL2 in human juvenile OGCT cases.²⁹ Using our previous *Foxl2* ChIP-on-Chip data from WT mouse ovaries,¹⁵ we conducted a similar analysis for potential enrichment in *Foxl2* targets among differentially expressed genes in mouse juvenile OGCT samples. Again, genes differentially expressed in the tumors were significantly enriched for *Foxl2* binding at their promoter regions (Figure 3).

Altogether, these results suggest that alterations in FOXL2 activity may have a central role in OGCT pathogenesis, whether through its mutation in adult-type or through its downregulation in juvenile-type OGCTs.

Misregulation of FOXL2 direct target genes in adult-type OGCT is likely to favor cell cycle progression and apoptosis inhibition

To focus on the effects of the p.Cys134Trp *FOXL2* mutation, we chose to study in more details the alterations in expression profile

of FOXL2 direct target genes in OGCT. For improved accuracy, we used the list of potential FOXL2 direct targets recently compiled from genome-wide data, both the above-mentioned ChIP-on-Chip¹⁵ and our previous transcriptomic study on human OGCT-derived KGN cells transiently overexpressing WT-FOXL2.¹³ The intersection of these datasets involves 1820 high-confidence target genes, whose names are listed in the Supplementary Table 1 of a previous study,¹⁵ and 1475 of which are part of our FSH non-responsive set. Next, we extracted from our OGCT microarray results data concerning genes directly regulated by FOXL2 to further study their behavior and understand the effect of the FOXL2 mutation on their expression.

To study the alterations of the expression patterns of FOXL2 target genes, we classified the direct targets into three groups depending of their behavior in control GCs compared with OGCTs, similarly to the global analysis, and clustered them using a *K*-means clustering approach with *K*=3 (Figure 2b). The clusters containing differentially expressed FOXL2 target genes involved 960 genes, 377 of which displayed a tendency to downregulation

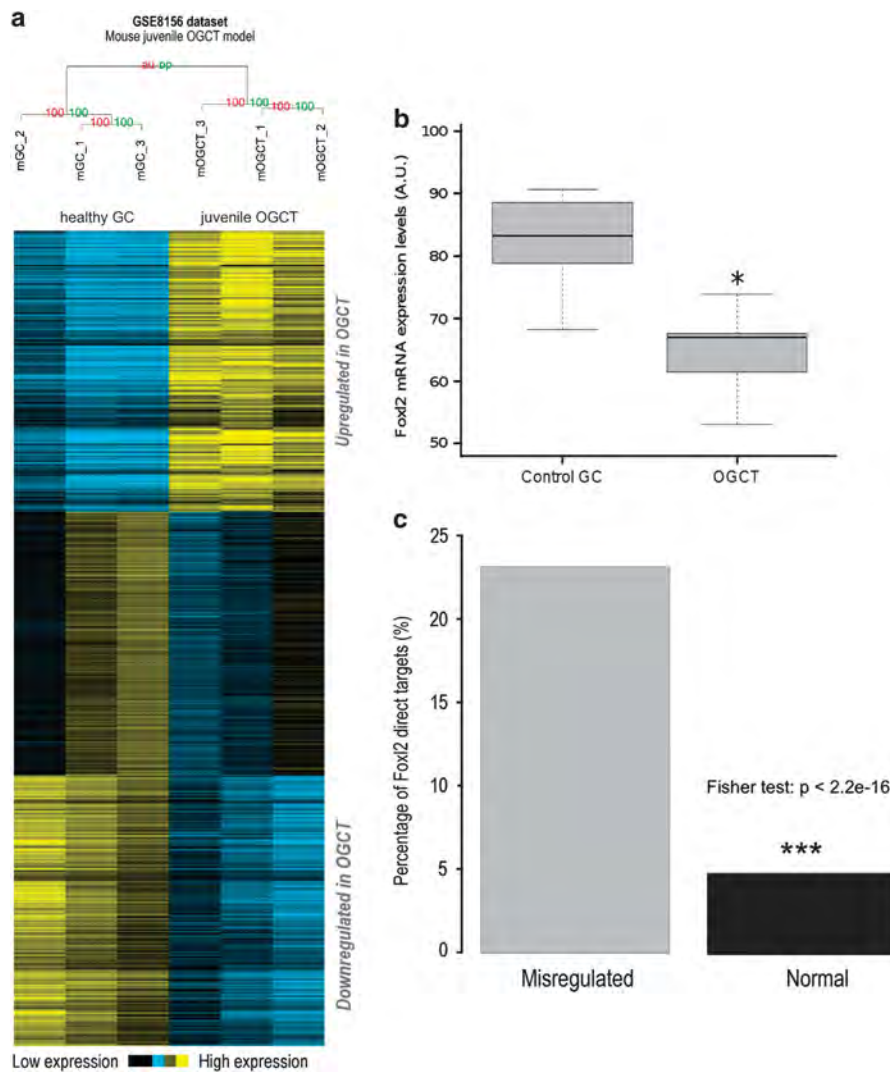


Figure 3. *K*-means clustering of published murine juvenile OGCT model and potential role of *Foxl2* downregulation. (a) Graphical output of *K*-means clustering analysis of the expressional behavior of murine transcripts from the *smad1-5-8* knockout mice model of juvenile OGCT (GSE8156), performed using Cluster3.0 (*K*=3, 500 tries, distance measure: Spearman rank correlation). (b) Relative levels of *Foxl2* mRNA according to microarray assessment of juvenile OGCT and healthy GC in the same mouse model. Statistical significance in Student *t*-test: **P*<0.05. Error bar represents 95% confidence interval. (c) Enrichment for *Foxl2* binding at the promoters of genes whose expression is differentially expressed in juvenile OGCT samples (clusters 1 and 3 from a). The hypergeometric distribution (Fisher's exact test) was used to compute the significance of the enrichment.

and 583 to upregulation in OGCT samples (Gene annotations corresponding to the differentially expressed genes can be found in Supplementary Table 2, with accompanying significance metrics).

Then, we performed a functional annotation with the DAVID Software, using the gene lists from the two pathology-relevant clusters (that is, containing up- or down-regulated FOXL2 target genes). FOXL2 direct targets that tend to be upregulated in OGCTs are significantly enriched for association with GO terms linked to cell proliferation (Figure 2c). This is consistent with the global pattern of gene misregulation that we observed for all genes (Figure 1b). Interestingly, we recently showed that FOXL2, through its action as a transcription factor, interferes with cell proliferation and inhibits progression through the cell cycle at the G1/S checkpoint through regulation of key cell cycle regulators.¹⁵ Moreover, previous studies have indicated that the p.Cys134Trp mutant would be rather hypomorphic on this category of genes (notably *GADD45A*, and indirectly on *CDKN2A*). Our analysis herein indicates that FOXL2 ability to regulate key genes linked to cell cycle regulation is indeed disturbed in OGCTs.

Interestingly, FOXL2 targets that tend to be downregulated in OGCTs, are significantly enriched for association with GO terms linked to apoptosis and cell cycle arrest (Figure 2d), which is once again consistent with the global gene misregulation pattern (Figure 1c). This is also consistent with the recent discovery of the reduced ability of the p.Cys134Trp FOXL2 mutant protein with regard to its ability to induce apoptosis of OGCT-derived cells.¹⁷ Indeed, our transcriptome data support the authors' hypothesis, linking a deficiency of the mutant protein in its ability to promote apoptosis to the malignant transformation process of GCs.

Molecular contribution of the p.Cys134Trp FOXL2 somatic mutation to OGCT-associated transcriptomic alterations

To further explore whether the p.Cys134Trp FOXL2 mutation is indeed a loss- or a gain-of-function mutation, we assessed the degree of misregulation of FOXL2 target genes by comparing the mean fluorescence values of gene probes in the control GC samples versus those measured in the OGCT samples.

For a first-pass analysis, we ranked all FOXL2 target genes according to the absolute amplitude of their differentially expression in OGCT samples compared with healthy GCs (from the most differentially expressed to the least differentially expressed). This list enabled us to use the GOrilla algorithm (<http://cbl-gorilla.cs.technion.ac.il>).³¹ This algorithm outputs GO terms that are significantly enriched at the top of a ranked list and discovers a relevant threshold to be determined by the dataset (that is, which is the lowest element in the list allowing significant enrichment for the term). Interestingly, among GO terms enriched at the top of the FOXL2 differentially expressed targets, GOrilla uncovered cellular response to stress (GO:0033554;

$P=1.92 \times 10^{-4}$) with a 3.15-fold enrichment in the top 89 differentially expressed genes, and negative regulation of cell proliferation (GO:0008285; 5.84×10^{-4}) with a 3.75-fold enrichment in the top 90 differentially expressed genes. This suggests the existence a misregulation of FOXL2 targets involved in GC homeostasis.

To gain further insights into this altered regulation, we then focused on a subset of FOXL2 direct target genes that had been confirmed by multiple lines of evidence (that is, genome-scale studies, RT-qPCR, ChIP-qPCR and/or luciferase assays) and that have been linked to some extent to cancer progression or cell stress response.^{13–15,32} Of these, 11 genes are not responsive to FSH, and 10 of these genes were significantly differentially expressed in OGCT samples as compared with GC samples (P -values < 0.05 in repeated one sample t -tests after the Bonferroni correction for multiple testing; Figure 2e). Interestingly, nine out of those ten behave in a manner that is compatible with a FOXL2 hypomorphy, that is, genes normally activated by FOXL2 are found significantly downregulated in OGCT samples (Figure 2e).

To better understand whether such misregulations could be linked to a loss of transactivation of the p.Cys134Trp FOXL2 mutant, we performed reporter assays using previously characterized FOXL2-responsive promoters from the differentially expressed gene list. We thus performed luciferase assays using the following available reporters: pSODluc-3340 for the *MnSOD* promoter and GADD45A-luc for the *GADD45A* promoter.^{5,15} We had previously observed that the WT and p.Cys134Trp mutant FOXL2 behaved similarly on these promoters in KGN cells, which are heterozygous for p.Cys134Trp mutation and whose transcriptome and proteome are likely to have adapted in response to the mutation.^{5,15} Here, however, we were able to detect the adult OGCT-associated mutant FOXL2 was slightly hypomorphic (~20% loss of transactivation) on the two reporters in both COV434 cells (OGCT-derived) and HeLa cells (cervical cancer-derived cells), which both have only WT FOXL2 alleles and low to null endogenous expression levels^{5,15} (Figure 4). Although the loss of activity is partial, such a defect on similar key stress response, apoptosis and cell cycle target genes over a long period of time might be responsible at least partly for the malignant transformation of healthy GCs into OGCT.

GENERAL DISCUSSION

The recent discovery of p.Cys134Trp FOXL2 mutation as being characteristic of adult OGCTs has opened new avenues for understanding the biology of this peculiar ovarian cancer.⁹ The presence of a single missense FOXL2 somatic mutation in over 95% of adult OGCTs⁹ suggests that it might be somehow driving and/or facilitating the malignant transformation of GCs. Before the discovery of the recurrent p.Cys134Trp FOXL2 mutation by an

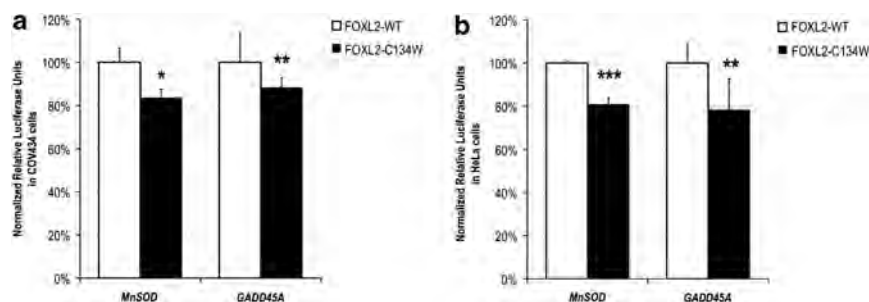


Figure 4. Reduced transactivation abilities of the p.Cys134Trp FOXL2 mutant on targets strongly differentially expressed in OGCT samples. Luciferase assays using pSODluc-3340³⁷ and GADD45A-luc³⁸ in (a) COV434 cells and (b) HeLa were performed as described previously.¹⁵ Relative Luciferase Units were calculated as previously, and then normalized to allow comparison of transactivation on different reporters. Error bars: s.d. Statistical significance in Student t -tests: * $P < 0.05$, ** $P < 0.01$ and *** $P < 0.001$.

unbiased whole-transcriptome sequencing approach,⁹ only one fact linking FOXL2 and OGCTs had been reported, that is, its reduced expression in juvenile-type samples.²⁹ With hindsight, however, this connection between FOXL2 and malignant transformation makes sense.¹⁸

Thus far, only a few unconnected clues as to how the p.Cys134Trp FOXL2 mutation might be linked to malignant transformation of GCs have been uncovered. These include its inefficiency at inducing GC apoptosis,¹⁷ a potential hyperactivity on the ovarian-specific aromatase promoter,¹⁹ a potentially disturbed functional interaction with SMAD3,⁵ and a hypomorphism on cell-cycle-related targets.¹⁵ Here, we used a whole transcriptome approach to identify molecular characteristics of the pathology, through the analysis of 10 OGCT samples exhibiting different clinical and histopathological characteristics, but all positive for the p.Cys134Trp mutation.⁶ We also analyzed comprehensively the mRNA expression profiles by i) comparing them to the best available control, that is, GC derived from healthy patients undergoing IVF protocols, as well as ii) using our prior knowledge on direct FOXL2 targets in GCs.¹⁵

Finally, the present analysis allows us to draw several conclusions on the molecular features of adult OGCT. First, the analyzed OGCT samples exhibit typical hallmarks of cancer-favoring cell cycling activity, but decreased sensitivity to cell death. Second, consistently with the preeminence of FOXL2 downregulation or mutation in OGCTs, we observe that differentially expressed genes are especially enriched for FOXL2 direct target genes, in a way that is predicted to promote malignant transformation (that is, reactivation of genes associated with cell cycling, downregulation genes associated with cell death, and so on). Third, current results support the hypothesis that the p.Cys134Trp FOXL2 mutation causes a partial loss-of-function, which is the hallmark of a tumor suppressor. Indeed, the mutant FOXL2 protein acts in an hypomorphic manner on key FOXL2 target genes and/or regulated processes.^{15,17} This is consistent with what we observe here in OGCT samples, that is, that normally activated targets are mostly downregulated, and, reciprocally, inhibited targets are reactivated. This tendency should not emerge if this mutation corresponded to a plain gain-of-function.

Altogether, the forkhead transcription factor FOXL2 has a central role in OGCT pathogenesis, whether through the p.Cys134Trp mutation in adult cases or through its downregulation in juvenile cases. Unraveling the molecular characteristics of OGCTs, and how the mutation interferes with the normal GC homeostasis and causes malignant transformation, will hopefully open the way to develop targeted therapeutic strategies for the OGCT patients.

MATERIALS AND METHODS

Adult ovarian granulosa cell tumor sample selection

We obtained tumor samples from patients treated and operated at the Helsinki University Central Hospital (Helsinki, Finland), as well as two ethnically matched primary GC samples derived from IVF programs. Following OGCT diagnosis, tumor tissue was processed as previously.³³ The p.Cys134Trp mutation status of FOXL2 was analyzed as described.⁶ The ethical committee of Helsinki University Central Hospital and the National Supervisory Authority for Welfare and Health in Finland approved the OGCT study as a whole. Informed consent from all patients enrolled in the study was obtained.

RNA extraction, cDNA synthesis and microarray analysis

350 ng total RNA extracted from tissue samples was reverse-transcribed and linearly amplified using the Whole Transcriptome Amplification Transplex kit (Sigma-Aldrich, St Louis, MO, USA), according to the manufacturer's instructions. The amplified cDNAs from the 12 samples (2 primary GC controls and 10 tumor samples) were sent to the Nimblegen expression platform (Roche NimbleGen, Reykjavik, Iceland) in technical

duplicates (independent reverse transcriptions, amplifications and hybridization per RNA sample). The design of the array that was used is the high-density Human Expression 12 × 135K array set, that allows the study of 12 samples in parallel, interrogating over 45K annotated transcripts of HG18 assembly. Nimblegen performed sample labeling, hybridization and fluorescence acquisition, and then provided us with normalized data files. Raw files were deposited at the Array Express repository, under accession number E-MTAB-483.

Transcriptome data processing and statistical analyses

Raw data from mouse FSH-treated GCs (accession GSE20466)²¹ and the juvenile OGCT models (GSE8156)³⁰ were downloaded from the GEO Datasets repository, and RMA normalization was applied to the samples. Significance analysis of microarray²² was performed on the FSH-treatment dataset using its implementation in the R software (<http://www.r-project.org/>) through the *siggenes* package. Significantly regulated genes were found by adjusting delta values to reach the 5% false discovery rate threshold.

Data processing from the human OGCT transcriptome was performed in the R software, using packages *preProcessCore* and recently published batch-correction algorithm *ComBat*.²⁰ Briefly, transcriptomes having passed Nimblegen quality control in batch 1 and batch 2 of hybridizations were imported into R, probe fluorescence values were averaged per gene, transformed into log₂ space, subjected to quantile normalization and batch effects adjustment, as recommended for this type of studies.³⁴ FSH-responsive genes were then identified and eliminated from further analyses.

To estimate the homogeneity of tumors and reliability of replicates, sample clustering was performed using the *Pvclust* algorithm,²³ using its R package implementation. Parameters chosen for the clustering step were the Pearson correlation coefficient as a similarity measure, and the use of complete linkage hierarchical clustering. To estimate robustness and *P*-values, experiments were conducted with 10,000 bootstrap replications of the clustering step.

Gene clustering was performed using the stand-alone java version of the Cluster 3.0 libraries. Before clustering, data was log-transformed when necessary and centered to mean. *K*-means clustering was then performed using Spearman rank correlation as distance measure, a *K* of 3 and 500 tries.

Statistics and functional annotation of gene lists

Statistical tests to assess the significance of overlaps and differences were performed using basic packages of the R statistical software. Functional annotation of gene lists were performed by converting gene identifiers to their 'Entrez gene ID' identifier using the BioMart portal (www.biomart.org/), then using the DAVID functional annotation software.^{25,26} For each list, we analyzed the enrichments computed by DAVID for Gene Ontology Biological Process terms. On ranked genes lists, we used the Gorilla algorithm (<http://cbl-gorilla.cs.technion.ac.il/>) to compute enrichment analyses in top differentially expressed genes.³¹ Analysis for FOXL2 ChIP peak enrichments among OGCT differentially expressed genes was operated using the published peak files (E-MTAB-399 and E-MTAB-400 datasets), that were remapped to current assemblies hg19 and mm9 using the UCSC liftOver tool. Peaks were annotated to closest genes using scripts from the Homer suite.³⁵ Overlaps from lists were computed using an in-house Perl script.

Cell culture, transfections and luciferase assays

The human WT and C134W mutant FOXL2-GFP expression vectors were described previously.³⁶ The luciferase reporter plasmids pSODluc-3340 and GADD45A-luc used in this study were described previously.^{37,38} COV434 GCs³⁹ were grown in DMEM-F12, supplemented with 10% FBS and 1% penicillin/streptomycin (Life technologies, Grand Island, NY, USA). HeLa cells were grown in supplemented DMEM. COV434 and HeLa cells were plated 12 h before transfection, and transfected using the calcium phosphate method.⁴⁰ Relative luciferase units correspond to the ratio of Firefly over Renilla luciferase activity from at least six independent replicates.

CONFLICT OF INTEREST

The authors declare no conflict of interest.

ACKNOWLEDGEMENTS

We thank Dr Ralf Bützow and Dr Unkila-Kallio for help and collection of the human OGCT samples. We thank Dr Denis Mestivier for his advice on clustering analysis of the OGCT microarray samples. BAB was funded by AMN/Université Paris Diderot-Paris 7 fellowships. MA was funded by a grant from The Helsinki University Central Hospital Research Funds. NA and MH were funded by Academy of Finland, Sigrid Juselius Foundation and Helsinki University Central Hospital. DL was funded by Université Paris Diderot-Paris 7. MBB was funded by CNRS and Université Lyon 1. RAV was funded by Institut Universitaire de France, Fondation pour la Recherche Médicale, Ligue Nationale Contre le Cancer (Comité de Paris), Groupement d'Entreprises Françaises dans la Lutte contre le Cancer, CNRS and Université Paris VII. This work was supported by grants from Fondation pour la Recherche Médicale (FRM), from The Helsinki University Central Hospital Research Funds and from Academy of Finland, Sigrid Juselius Foundation and Helsinki University Central Hospital.

REFERENCES

- Pectasides D, Pectasides E, Psyrii A. Granulosa cell tumor of the ovary. *Cancer Treat Rev* 2008; **34**: 1–12.
- Schumer ST, Cannistra SA. Granulosa cell tumor of the ovary. *J Clin Oncol* 2003; **21**: 1180–1189.
- East N, Alobaid A, Goffin F, Ouallouche K, Gauthier P. Granulosa cell tumour: a recurrence 40 years after initial diagnosis. *J Obstet Gynaecol Can* 2005; **27**: 363–364.
- Kalfa N, Veitia RA, Benayoun BA, Boizet-Bonhoure B, Sultan C. The new molecular biology of granulosa cell tumors of the ovary. *Genome Med* 2009; **1**: 81.
- Benayoun BA, Caburet S, Dipietromaria A, Georges A, D'Haene B, Pandaranayaka PJ *et al*. Functional exploration of the adult ovarian granulosa cell tumor-associated somatic FOXL2 mutation p.Cys134Trp (c.402C>G). *PLoS One* 2010; **5**: e8789.
- Jamieson S, Butzow R, Andersson N, Alexiadis M, Unkila-Kallio L, Heikinheimo M *et al*. The FOXL2 C134W mutation is characteristic of adult granulosa cell tumors of the ovary. *Mod Pathol* 2010; **23**: 1477–1485.
- Kim MS, Hur SY, Yoo NJ, Lee SH. Mutational analysis of FOXL2 codon 134 in granulosa cell tumour of ovary and other human cancers. *J Pathol* 2010; **221**: 147–152.
- Schrader KA, Gorbacheva B, Senz J, Heravi-Moussavi A, Melnyk N, Salamanca C *et al*. The specificity of the FOXL2 c.402C>G somatic mutation: a survey of solid tumors. *PLoS One* 2009; **4**: e7988.
- Shah SP, Kobel M, Senz J, Morin RD, Clarke BA, Wiegand KC *et al*. Mutation of FOXL2 in granulosa-cell tumors of the ovary. *N Engl J Med* 2009; **360**: 2719–2729.
- Crisponi L, Deiana M, Loi A, Chiappe F, Uda M, Amati P *et al*. The putative forkhead transcription factor FOXL2 is mutated in blepharophimosis/ptosis/epicanthus inversus syndrome. *Nat Genet* 2001; **27**: 159–166.
- Cocquet J, Pailhoux E, Jaubert F, Servel N, Xia X, Pannetier M *et al*. Evolution and expression of FOXL2. *J Med Genet*. 2002; **39**: 916–921.
- Uhlenhaut NH, Jakob S, Anlag K, Eisenberger T, Sekido R, Kress J *et al*. Somatic sex reprogramming of adult ovaries to testes by FOXL2 ablation. *Cell* 2009; **139**: 1130–1142.
- Batista F, Vaiman D, Dausset J, Fellous M, Veitia RA. Potential targets of FOXL2, a transcription factor involved in craniofacial and follicular development, identified by transcriptomics. *Proc Natl Acad Sci USA* 2007; **104**: 3330–3335.
- Benayoun BA, Batista F, Auer J, Dipietromaria A, L'Hote D, De Baere E *et al*. Positive and negative feedback regulates the transcription factor FOXL2 in response to cell stress: evidence for a regulatory imbalance induced by disease-causing mutations. *Hum Mol Genet* 2009; **18**: 632–644.
- Benayoun BA, Georges AB, L'Hote D, Andersson N, Dipietromaria A, Todeschini AL *et al*. Transcription factor FOXL2 protects granulosa cells from stress and delays cell cycle: role of its regulation by the SIRT1 deacetylase. *Hum Mol Genet* 2011; **20**: 1673–1686.
- Lee K, Pisarska MD, Ko JJ, Kang Y, Yoon S, Ryou SM *et al*. Transcriptional factor FOXL2 interacts with DP103 and induces apoptosis. *Biochem Biophys Res Commun* 2005; **336**: 876–881.
- Kim JH, Yoon S, Park M, Park HO, Ko JJ, Lee K *et al*. Differential apoptotic activities of wild-type FOXL2 and the adult-type granulosa cell tumor-associated mutant FOXL2 (C134W). *Oncogene* 2011; **30**: 1653–1663.
- Benayoun BA, Kalfa N, Sultan C, Veitia RA. The forkhead factor FOXL2: a novel tumor suppressor? *Biochim Biophys Acta* 2010; **1805**: 1–5.
- Fleming NI, Knower KC, Lazarus KA, Fuller PJ, Simpson ER, Clyne CD. Aromatase is a direct target of FOXL2: C134W in granulosa cell tumors via a single highly conserved binding site in the ovarian specific promoter. *PLoS One* 2010; **5**: e14389.
- Johnson WE, Li C, Rabinovic A. Adjusting batch effects in microarray expression data using empirical Bayes methods. *Biostatistics* 2007; **8**: 118–127.
- Nagaraja AK, Middlebrook BS, Rajanahally S, Myers M, Li Q, Matzuk MM *et al*. Defective gonadotropin-dependent ovarian folliculogenesis and granulosa cell gene expression in inhibin-deficient mice. *Endocrinology* 2010; **151**: 4994–5006.
- Tusher VG, Tibshirani R, Chu G. Significance analysis of microarrays applied to the ionizing radiation response. *Proc Natl Acad Sci USA* 2001; **98**: 5116–5121.
- Suzuki R, Shimodaira H. Pvcust: an R package for assessing the uncertainty in hierarchical clustering. *Bioinformatics* 2006; **22**: 1540–1542.
- Saldanha AJ. Java Treeview—extensible visualization of microarray data. *Bioinformatics* 2004; **20**: 3246–3248.
- Dennis Jr G, Sherman BT, Hosack DA, Yang J, Gao W, Lane HC *et al*. DAVID: database for annotation, visualization, and integrated discovery. *Genome Biol*. 2003; **4**: P3.
- Huangda W, Sherman BT, Lempicki RA. Systematic and integrative analysis of large gene lists using DAVID bioinformatics resources. *Nat Protoc* 2009; **4**: 44–57.
- Hanahan D, Weinberg RA. The hallmarks of cancer. *Cell* 2000; **100**: 57–70.
- Hanahan D, Weinberg RA. Hallmarks of cancer: the next generation. *Cell* 2011; **144**: 646–674.
- Kalfa N, Philibert P, Patte C, Ecochard A, Duvillard P, Baldet P *et al*. Extinction of FOXL2 expression in aggressive ovarian granulosa cell tumors in children. *Fertil Steril* 2007; **87**: 896–901.
- Pangas SA, Li X, Umans L, Zwijsen A, Huylebroeck D, Gutierrez C *et al*. Conditional deletion of Smad1 and Smad5 in somatic cells of male and female gonads leads to metastatic tumor development in mice. *Mol Cell Biol* 2008; **28**: 248–257.
- Eden E, Navon R, Steinfeld I, Lipson D, Yakhini Z. GOrilla: a tool for discovery and visualization of enriched GO terms in ranked gene lists. *BMC Bioinformatics* 2009; **10**: 48.
- Blount AL, Schmidt K, Justice NJ, Vale WW, Fischer WH, Bilezikjian LM. FoxL2 and Smad3 coordinately regulate follistatin gene transcription. *J Biol Chem* 2009; **284**: 7631–7645.
- Kyronlahti A, Kauppinen M, Lind E, Unkila-Kallio L, Butzow R, Klefstrom J *et al*. GATA4 protects granulosa cell tumors from TRAIL-induced apoptosis. *Endocr Relat Cancer* 2010; **17**: 709–717.
- Chen C, Grennan K, Badner J, Zhang D, Gershon E, Jin L *et al*. Removing batch effects in analysis of expression microarray data: an evaluation of six batch adjustment methods. *PLoS One* 2011; **6**: e17238.
- Heinz S, Benner C, Spann N, Bertolino E, Lin YC, Laslo P *et al*. Simple combinations of lineage-determining transcription factors prime cis-regulatory elements required for macrophage and B cell identities. *Mol Cell* 2010; **38**: 576–589.
- Moumne L, Dipietromaria A, Batista F, Kocer A, Fellous M, Pailhoux E *et al*. Differential aggregation and functional impairment induced by polyalanine expansions in FOXL2, a transcription factor involved in cranio-facial and ovarian development. *Hum Mol Genet* 2008; **17**: 1010–1019.
- Kim HP, Roe JH, Chock PB, Yim MB. Transcriptional activation of the human manganese superoxide dismutase gene mediated by tetradecanoylphorbol acetate. *J Biol Chem* 1999; **274**: 37455–37460.
- Rishi AK, Sun RJ, Gao Y, Hsu CK, Gerald TM, Sheikh MS *et al*. Post-transcriptional regulation of the DNA damage-inducible gadd45 gene in human breast carcinoma cells exposed to a novel retinoid CD437. *Nucleic Acids Res* 1999; **27**: 3111–3119.
- Zhang H, Vollmer M, De Geyter M, Litzstorf Y, Ladewig A, Durrenberger M *et al*. Characterization of an immortalized human granulosa cell line (COV434). *Mol Hum Reprod* 2000; **6**: 146–153.
- Sambrook J, Russell DW. *Molecular Cloning – A Laboratory Manual*. 3 edn. Cold Spring Harbor Laboratory Press: New York, 2001.

Supplementary Information accompanies the paper on the Oncogene website (<http://www.nature.com/onc>)